 Bull. Chem. Soc. Jpn. Vol. 84, No. 1, 125–131 (2011)

Improvement of Carbon-Based Counter Electrode for Dye-Sensitized Solar Cells

Sho Sakurai,[1] Hai-qing Jiang,[2] Masashi Takahashi,[1] and Koichi Kobayashi*[1,2]

[1]Department of Chemistry and Energy Engineering, Tokyo City University, Tokyo 158-8557

[2]Research Center for Energy and Environmental Science, Advance Research Laboratory, Tokyo City University, Tokyo 158-0082

Received August 26, 2010; E-mail: kkobaya@tcu.ac.jp

A ClO_4^--doped poly(3,4-ethylenedioxythiophene) (PEDOT)-supported carbon particle (PEDOT–ClO_4^-/C) composite film electrode was prepared by electrophoretic deposition on transparent conductive oxide glass to improve the performance of carbon-based counter electrodes for dye-sensitized solar cells (DSSC). Evaluation of the electrochemical impedance demonstrated that the PEDOT–ClO_4^-/C composite film electrode had a lower iodide electrolyte/electrode interfacial resistance than that of a simple carbon particle film electrode. As a result, a DSSC with a PEDOT–ClO_4^-/C composite film counter electrode had a significantly improved fill factor and photovoltaic conversion efficiency, compared to a cell based on a simple carbon particle film electrode. Furthermore, the photovoltaic conversion efficiency of a DSSC with a PEDOT–ClO_4^-/C composite film electrode demonstrated approximately 85% of the conversion efficiency of a DSSC with a platinum-sputtered glass counter electrode.

In recent years we have faced significant energy problems, such as the dwindling supply of fossil fuels and global warming caused by the emission of greenhouse effect gases. As one solution to these energy problems, we could make far better use of our constant, inexhaustible supply of solar energy. Therefore, solar cells that can convert solar energy to electric energy are expected to be used as a future source of clean energy. Of all solar cells, dye-sensitized solar cells (DSSCs) have attracted increased interest because they can be prepared at a lower production cost through a simpler production process than conventional silicon-type solar cells.[1,2]

A typical DSSC is composed of a working electrode with a nanocrystalline TiO_2 layer containing a chemically adsorbed sensitizer dye on fluorine-doped tin oxide (FTO) glass, a redox electrolyte for reduction of the sensitizer dye that emits electrons by photoexcitation, and a counter electrode for reduction of the electrolyte by electrons that pass through an external circuit. Currently, platinum sputtered on a glass substrate is widely used as a counter electrode material, because platinum has good electrical conductivity, a high catalytic activity for the I^-/I_3^- redox couple in the electrolyte, and high chemical stability in the presence of iodine. Unfortunately, platinum is very expensive and its supply is limited. Therefore, the development of alternative counter electrode materials is highly desirable for the commercialization of DSSCs.

In recent years, several studies of DSSCs have employed carbonaceous materials[3–7] such as carbon nanotubes, carbon black, graphite, and organic conductive polymers[8–13] such as PEDOT–ClO_4^- and polypyrrole as a counter electrode material. Carbonaceous materials are quite attractive due to their high electric conductivity, corrosion resistance toward iodine, catalytic activity for the reduction of triiodide ion and low cost. However, there also is a disadvantage in that the contact between carbon particles and FTO glass is very poor.

On the other hand, electrochemical deposition has been used for preparing a uniform and compact film. As the film thickness obtained by this process could be easily and in a short time controlled by electrochemical duration and applied electric field intensity, the obtained film has more uniform and compact structure compared with that prepared by other conventional processes. Among electrochemical deposition, electrophoretic deposition is a very simple and easy method for preparing a uniform and compact particulate film. This uniform structure is favorable to the improvement of electron transfer due to increase of specific surface area, resulting in the improvement of performance. Also, electropolymerization could easily be used to prepare an ultrathin and homogenous conductive polymer film with little impurity on the surface of C particles. Accordingly, it is expected that PEDOT–ClO_4^-/C composite film modified by forming C network structure by covering the C particles with PEDOT–ClO_4^- would exhibit higher performance as counter electrode material than that by the other ordinary protocols.

In the present study, we attempted to prepare a PEDOT–ClO_4^-/C composite film by electrochemical deposition, and to further improve the performance of carbon particle film electrodes. The resulting PEDOT–ClO_4^-/C composite film electrodes were characterized by cyclic voltammetry (CV) and electrochemical impedance spectroscopy (EIS). Cell performance was evaluated using current–voltage (I–V) measurements. In addition, we focused on a construction of good adhesion between C particles and the conductive glass electrode.

Experimental

Preparation of a PEDOT–ClO_4^-/C Composite Film Counter Electrode. A PEDOT–ClO_4^-/C composite film

Published on the web January 1, 2011; doi:10.1246/bcsj.20100239

was fabricated on a counter electrode by electrophoretic deposition.[14] In order to provide a high dispersion of carbon black (C), poly(vinylpyrrolidone) (PVP, MW: 10000, Tokyo Kasei Co., Ltd.) was used as a capping agent.[15] The suspension of C particles was ultrasonically dispersed by adding the C particles (Printex L-6, Degussa) into a 3 wt% PVP ethanol solution. A PVP-capped C particle suspension at a weight ratio of C/PVP = 0.66 was obtained. Two parallel pieces of FTO conductive glass substrate (Asahi Glass Co., Ltd., Japan) of the same size as the electrodes were immersed in the PVP-capped C particle suspension. After applying a 10 V DC bias voltage for 15 s, a C particle film was electrochemically deposited on the cathode surface. This film was then dried at 100 °C. The EDOT monomer was electrochemically polymerized to form a PEDOT–ClO_4^- layer on the surface of the C particles, after applying a 3.5 V DC voltage for various times (15, 30, and 60 s). Finally, a PEDOT–ClO_4^-/C/FTO CE was obtained after drying at 100 °C for 5 min. In comparison, a PEDOT–ClO_4^-/FTO CE was electrochemically prepared by immersing two parallel pieces of FTO conductive glass into the EDOT solution. A PEDOT–ClO_4^- layer was formed on the anode after applying a 3.5 V DC voltage for 15 s.

CE Characterization. PEDOT–ClO_4^- deposition was confirmed by X-ray photoelectron spectroscopy (XPS) using an SSX-100 system. Cross-sectional images of an electrode were obtained using a Hitachi S-400 FESEM system.

To further understand the photocurrent behavior of the DSSCs, EIS of the electrochemical cells with PEDOT–ClO_4^-/C/FTO glass (or PEDOT–ClO_4^-/FTO glass) electrodes was performed over a frequency range of 10^{-1}–10^6 Hz with an AC amplitude of 150 mV using a potentiostat (versaSTAT3, Princeton Applied Research, USA). A deposited Pt film electrode was used as a CE. The electrolyte used for the measurements of *I–V* and EIS consisted of 0.05×10^{-3} mol dm^{-3} I_2 (Wako, Japan), 0.5×10^{-3} mol dm^{-3} LiI (Wako, Japan), and 0.5×10^{-3} mol dm^{-3} 4-*t*-butylpyridine (Aldrich, USA) in 3-methoxypropionitrile (Tokyo Chemical Industry, Japan). The surface area of the electrochemical cell was 0.5024 cm^2, and the distance between the working electrode (WE) and the CE was maintained at 50 μm, which is similar to that of the sample fabricated for the measurement of *I–V* curves.

CV curves were obtained in an acetonitrile electrolyte solution containing 1×10^{-3} mol dm^{-3} I_2, 5×10^{-3} mol dm^{-3} LiI, and 0.1 mol dm^{-3} $LiClO_4$ at a scan rate of 100 mV s^{-1} from −0.5 to 1.5 V using a potentiostat. The electrochemical cell was composed of PEDOT–ClO_4^-/C/FTO WE (or PEDOT–ClO_4^-/FTO, Pt film), a Pt-film CE prepared by sputter deposition, and an Ag/AgI reference electrode. The distance between the two electrodes in the electrochemical cell was maintained at 5 mm, and the surface area of the electrode was 0.64 cm^2.

Preparation of Working Electrode for *I–V* Measurement. A photoanode was fabricated by electrophoretic deposition. Two parallel pieces of FTO conductive glass substrate (Asahi Glass Co., Ltd., Japan) of the same size as the electrodes were immersed in a TiO_2 suspension. After applying a 10 V DC bias voltage for 35 s, a TiO_2 particle film was electrochemically deposited on the cathode surface, which was then sintered at 500 °C for 30 min. The obtained TiO_2 particle film was immersed into a 0.3 mM N719 dye (Peccell Technologies Inc., Japan) solution at 40 °C for 2 h. The N719 dye solution was prepared by dissolving N719 dye into a mixture of *t*-butyl alcohol (Wako, Japan), ethanol (Wako, Japan), and acetonitrile (Wako, Japan) at a molar ratio of 1:1:2. Two-electrode sandwich DSSCs were fabricated according to a procedure given elsewhere. The distance between the WE and the CE was maintained at 50 μm, and the surface area of the DSSCs was 0.24 cm^2. The performance of the prepared DSSCs was measured using a 500 W Xe lamp light source and an AM 1.5 solar simulator (100 mW cm^{-2}).

Results and Discussion

Characterization of the As-Prepared Counter Electrode. The as-prepared PEDOT–ClO_4^-/C composite film counter electrodes were characterized by XPS measurements. Figure 1 shows XP spectra of C particle film, PEDOT–ClO_4^- film, and PEDOT–ClO_4^-/C composite film counter electrodes. As shown in Figure 1a, $S_{2p_{1/2}}$ and $S_{2p_{3/2}}$ peaks were observed at 165.3 and 164.0 eV for all samples except the C particle film. The $S_{2p_{1/2}}$ and $S_{2p_{3/2}}$ peak intensities increased linearly with increasing electropolymerization time, indicating that ordinary regular deposition of PEDOT–ClO_4^- occurred on the surface of the carbon particles. Furthermore, Figure 1b indicates an N_{1s} peak originating from nitrogen atoms in the PVP. As seen in Figure 1b, the highest nitrogen peak was observed for the PVP-capped C particle film, whereas no nitrogen peak was observed for the PEDOT–ClO_4^- composite film. Furthermore, the nitrogen peak of the PVP-capped C particle film was found to decrease with increasing electropolymerization time. This suggests that the surface of the PVP-capped C particle film was covered with a PEDOT–ClO_4^- film.

Figure 2 shows typical cross-sectional FE-SEM images of PEDOT–ClO_4^-, carbon particle, and PEDOT–ClO_4^-/C composite films on FTO glass electrodes. As shown in Figure 2, the surface of the FTO glass was densely covered by the C particle film, with a thickness of about 1 μm. No boundary between the PEDOT–ClO_4^- film and the PVP-capped C particle film was observed in the SEM images. However, the presence of fibrous polymer on the particle films was observed on the FTO glass electrode and C particle film surfaces (Figures 2a and 2c–2e). It was obvious that the surfaces of the C particle films on the FTO glass electrodes were homogeneously covered with thin PEDOT–ClO_4^- film. In a previous study,[8] chemical polymerization was applied to prepare a homogenous deposition of thin EDOT–ClO_4^- film on an FTO glass electrode. In this case, inhomogeneous lumps of PEDOT–ClO_4^- film on the surfaces of FTO glass electrodes and C particle films on FTO glass electrodes were observed. Therefore, electrophoretic deposition was highly effective for the homogenous deposition of a PEDOT–ClO_4^- film, compared with the previous chemical polymerization method.

Electrochemical Evaluation by Cyclic Voltammetry. The primary roles of the counter electrode are the reduction of I_3^- to I^- in the electrolyte and the collection of electrons from the external circuit. Therefore, it is necessary to investigate the electrocatalytic activity for the I^-/I_3^- redox reaction of the as-prepared counter electrodes. Figure 3 shows cyclic voltammograms of various electrochemical cells, the parameters of which

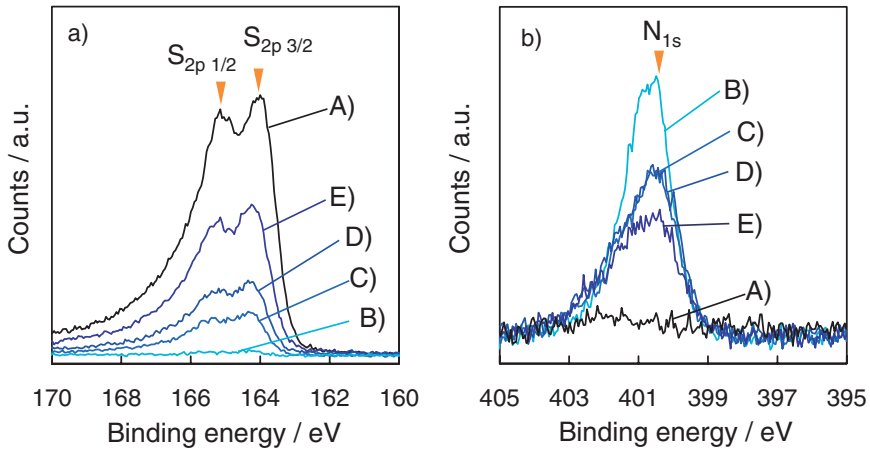

Figure 1. XP spectra of various electrode surfaces in the range of S_{2p} (a) and of N_{1s} (b) orbital peaks. A) PEDOT–ClO_4^-(3.5 V, 15 s) film on FTO glass electrode, B) C particle film on FTO glass electrode, C) PEDOT–ClO_4^-(3.5 V, 15 s)/C composite film on FTO glass electrode, D) PEDOT–ClO_4^-(3.5 V, 30 s)/C composite film on FTO glass electrode, E) PEDOT–ClO_4^-(3.5 V, 60 s)/C composite film on FTO glass electrode. All of the C particle layers were prepared on FTO glass electrodes by electrophoretic deposition (10 V for 15 s).

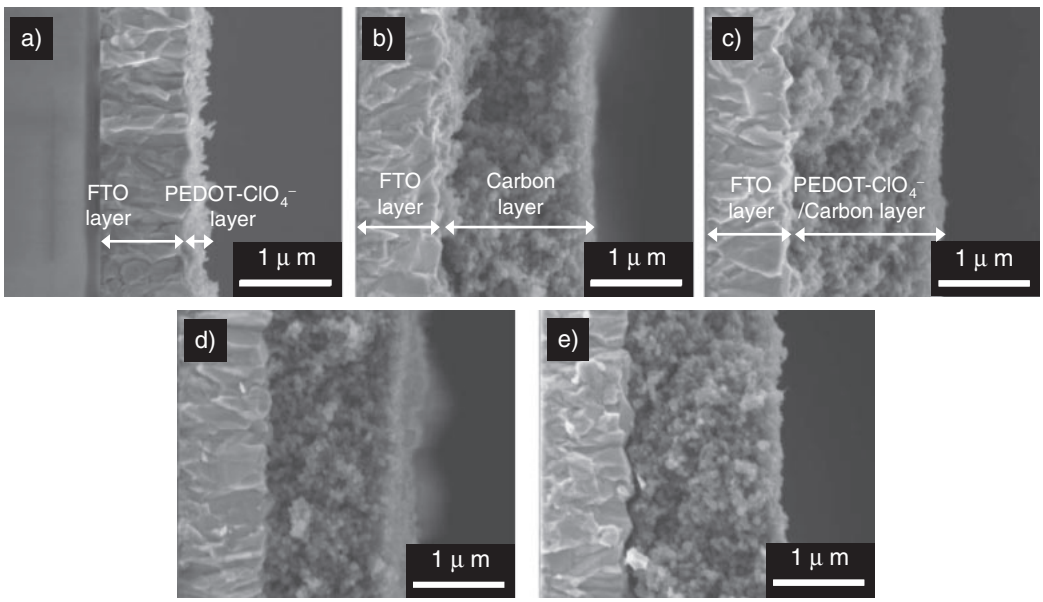

Figure 2. Cross-sectional FE-SEM images of various electrodes. a) PEDOT–ClO_4^-(3.5 V, 15 s) film on FTO glass electrode, b) C particle film on FTO glass electrode, c) PEDOT–ClO_4^-(3.5 V, 15 s)/C composite film on FTO glass electrode, d) PEDOT–ClO_4^-(3.5 V, 30 s)/C composite film on FTO glass electrode, e) PEDOT–ClO_4^-(3.5 V, 60 s)/C composite film on FTO glass electrode. All of the C particle films were prepared at an applied voltage of 10 V for 15 s by electrophoretic deposition.

are summarized in Table 1. As can be seen in Figure 3, the oxidation and reduction peaks of I_3^-/I^- on these CEs were roughly similar. Furthermore, there were two pairs of redox peaks for all electrodes, which were assigned to the chemical reactions below:

$$I_3^- + 2e^- = 3I^- \quad (1)$$

$$3I_2 + 2e^- = 2I_3^- \quad (2)$$

From the reduction current corresponding to the above eq 1, the maximum current densities of the C particle film and PEDOT–ClO_4^-(3.5 V, 15 s)/C composite film electrodes were 2.61 and 2.47 mA cm^{-2}, respectively, while the maximum current density of the PEDOT–ClO_4^-(3.5 V, 15 s) film electrode directly electropolymerized on the FTO glass electrode was 2.13 mA cm^{-2}. The higher current density of the PEDOT–ClO_4^-(3.5 V, 15 s)/C composite film electrode arose from an increase in reaction area resulting from the higher roughness of the C particle film, compared with that of the PEDOT–ClO_4^-(3.5 V, 15 s) film electrode. The current density for this reduction drastically increased after extending the reaction time to 60 s. The reduction current density increased from 2.47 mA cm^{-2} for the PEDOT–ClO_4^-(3.5 V, 15 s)/C composite film electrode to 3.15 mA cm^{-2} for the PEDOT–ClO_4^-(3.5 V, 60 s)/C composite film electrode. This increase was assumed to be caused by a decrease in the interfacial resistance between the carbon black and the electrolyte.

Table 1. Cyclic Voltammogram Parameters of Electrochemical Cells with Various Electrodes

	Ox peak curr. /mA cm^{-2}	Red peak curr. /mA cm^{-2}	Ox peak pot. /mV	Red peak pot. /mV	ΔE /mV
Pt	1.84	1.41	677	340	168.5
PEDOT–ClO_4^-(3.5 V, 15 s)	2.36	2.13	616	400	108.0
CB	2.64	2.61	736	299	218.5
PEDOT–ClO_4^-(3.5 V, 15 s)/CB	2.53	2.47	657	360	148.5
PEDOT–ClO_4^-(3.5 V, 30 s)/CB	2.74	2.83	637	360	138.5
PEDOT–ClO_4^-(3.5 V, 60 s)/CB	2.94	3.15	657	380	138.5

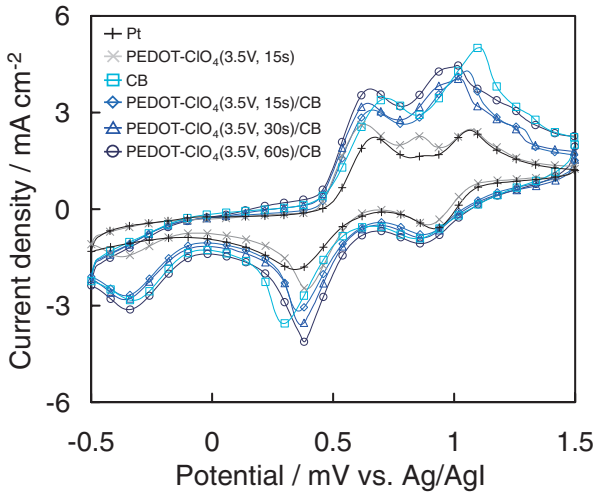

Figure 3. Cyclic voltammograms of various electrochemical cells. Electrochemical cells were constructed as a three-electrode system equipped with a conventional working electrode, a Pt-sputtered glass counter electrode, and an Ag/AgI reference electrode. The CV measurements were carried out at a scan rate of 100 mV s^{-1} in the range of −0.5 to 1.5 V.

On the other hand, a peak change in the redox potential was observed. The oxidation and reduction peak potentials of the C particle film electrode were 736 and 299 mV, respectively, while the oxidation and reduction peak potentials of the PEDOT–ClO_4^-(3.5 V, 15 s)/C composite film electrode were 657 and 360 mV, respectively. The potential difference between the oxidation and reduction peaks was 437 mV for the C particle film electrode and 297 mV for the PEDOT–ClO_4^-(3.5 V, 15 s)/C composite film electrode. This peak difference suggests a decrease in the overpotential of the iodide/triiodide redox reaction. Accordingly, the as-prepared electrode showed higher cathode performance than that of the C particle film electrode.

EIS Evaluation of As-Prepared Counter Electrodes. Electrochemical impedance experiments were performed to estimate the interfacial resistance between the electrodes and the electrolytes. The electrochemical impedance spectra are shown in Figure 4. Figure 4a shows Nyquist plots for electrochemical cells with PEDOT–ClO_4^- film and PEDOT–ClO_4^-/C composite film electrodes in the frequency range of 10^{-1}–10^6 Hz. Figures 4b and 4c show Bode diagrams of the serial resistance and phase angle differences between electrochemical cells with various WEs and a Pt-sputtered glass counter electrode, respectively. In the Nyquist plots of Figure 4a, three semicircular arcs can be clearly observed. Two semicircular arcs were observed for the Pt electrode. Furthermore, three characteristic frequencies were observed in the Bode phase plots of Figure 4c for electrochemical cells with a PEDOT–ClO_4^- film electrode and a PEDOT–ClO_4^-/C composite film electrode, which is similar to a previously reported PEDOT–ClO_4^-/TiO_2/FTO electrode.

The resistance of the as-prepared counter electrode was estimated from an equivalent circuit for solar cells with various WEs. Figure 5 shows a schematic representation of an equivalent circuit for this type of electrochemical cell.[16–20]

The impedance parameters were obtained by fitting the experimental spectra to that of the equivalent circuit, and are summarized in Table 2. In our analysis, the semicircles in the frequency regions of 10^3–10^5, 1–10^3, and 10^{-1}–1 Hz were attributed to impedances related to charge transfer occurring at the Pt film/electrolyte interface, at the PEDOT–ClO_4^- film/electrolyte interface, and a finite-layer Nernst diffusion impedance within the electrolyte, respectively. Impedances over 10^6 Hz could not be measured due to instrument limitations.

As seen in Table 2, R_2 of the electrolyte/C particle film interface was 47.90 Ω cm^2, which was extremely high compared with the other systems, as seen in the Bode diagram of Figure 4b. This high resistance was considered to mainly influence the internal resistance of the cell. On the other hand, R_2 of the PEDOT–ClO_4^-(3.5 V, 15 s)/C composite film interface was 8.63 Ω cm^2, about one-fifth that of the C particle film/electrolyte interface. This indicates that the introduction of a slight amount of PEDOT–ClO_4^- greatly improved the performance of the cathode. In addition, the R_2 value decreased with increasing time of electrolysis.

As shown in Figure 4c, the relaxation time of the PEDOT–ClO_4^-(3.5 V, 15 s)/C composite film electrode was shorter than that of the C particle film electrode, and the phase difference also decreased, while the relaxation time for the PEDOT–ClO_4^-(3.5 V, 15 s)/C composite film electrode was longer than the PEDOT–ClO_4^-(3.5 V, 15 s) electrode and the phase difference was smaller. These results indicate that the introduction of PEDOT–ClO_4^- to the C particle film electrode led to the formation of new reaction sites, resulting in a change of the relaxation time. Therefore, the introduction of PEDOT–ClO_4^- may decrease the overpotential against I^-/I_3^- redox, resulting in a higher reaction rate. This higher reaction rate may be due to the conductivity of PEDOT–ClO_4^- over carbon black.

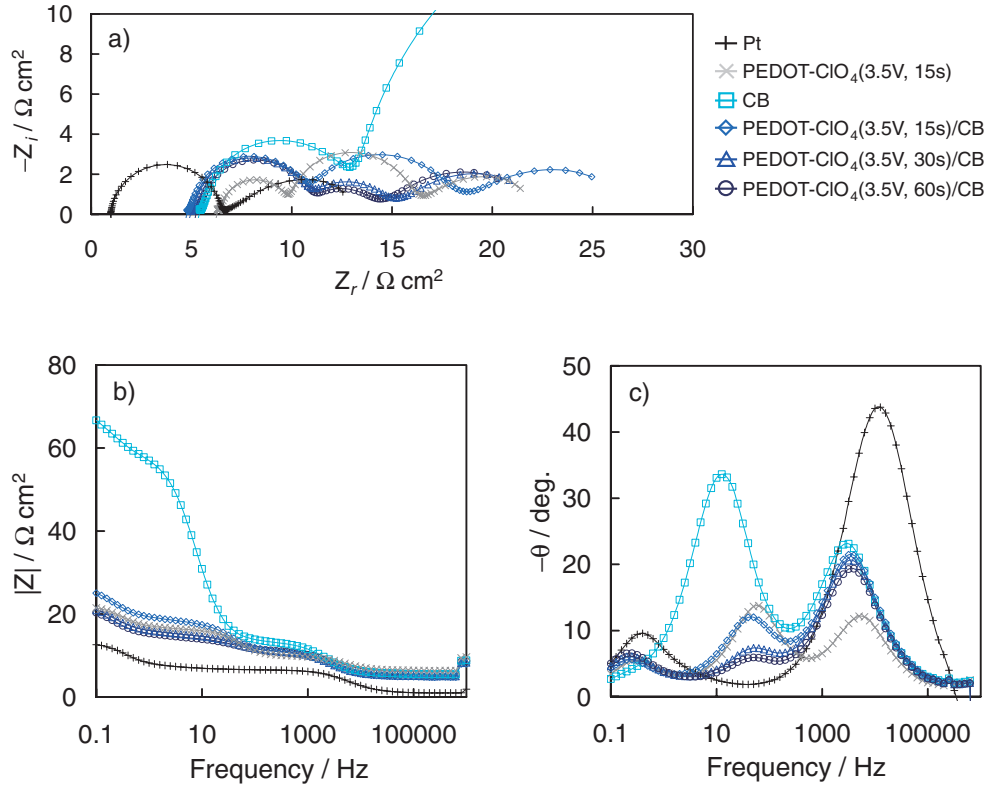

Figure 4. EIS spectra of electrochemical cells with various electrodes. a) Nyquist plots of electrochemical cells with various WEs and a Pt-sputtered glass counter electrode. b) Bode diagram of the serial resistance of the cells. c) Bode diagram of the phase angle differences of the cells. The measurements were carried out at an AC amplitude of 150 mV, in the range from 10^{-1} to 10^{6} Hz.

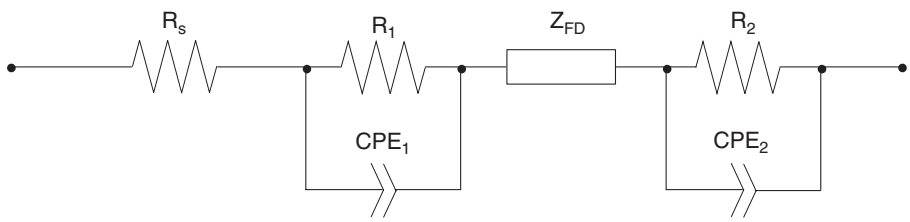

Figure 5. Equivalent circuit diagram of an electrochemical cell. R_s represents an ohmic series resistance element which contributes little to the interfacial reaction. R_1, R_2, and Z_{FD} represent the charge-transfer resistance at the Pt film/electrolyte interface, the charge-transfer resistance at the PEDOT–ClO_4^- film/electrolyte, C film/electrolyte, or PEDOT–ClO_4^-/C composite film/electrolyte interface, and the finite diffusion resistance of the electrolyte, respectively. CPE_1 and CPE_2 represent the constant phase elements at the Pt film/electrolyte interface and PEDOT–ClO_4^- film/electrolyte, C particle film/electrolyte, or PEDOT–ClO_4^-/C composite film/electrolyte interface, respectively.

Table 2. EIS Parameters of Electrochemical Cells with Various Electrodes

	R_s /Ω cm²	R_1 /Ω cm²	CPE_1 /μF cm^{-2}	n_1	R_2 /Ω cm²	CPE_2 /μF cm^{-2}	n_2
Pt	0.99	5.59	5.69	0.927	—	—	—
PEDOT–ClO_4^-(3.5 V, 15 s)	6.34	3.57	11.20	0.979	6.67	475.9	0.950
CB	5.52	7.75	12.95	0.969	47.90	526.6	0.856
PEDOT–ClO_4^-(3.5 V, 15 s)/CB	4.88	6.06	13.15	0.971	8.63	583.1	0.768
PEDOT–ClO_4^-(3.5 V, 30 s)/CB	4.99	6.04	13.20	0.953	5.34	748.4	0.695
PEDOT–ClO_4^-(3.5 V, 60 s)/CB	5.31	5.79	13.77	0.958	4.55	879.2	0.653

On the other hand, the decrease in the phase difference of PEDOT–ClO_4^-(3.5 V, 15 s)/C composite film compared to PEDOT–ClO_4^- film was caused by charge transfer of electrons in the carbon particle film electrode. As the electron conductivity of conductive polymer is higher than that of carbon black, the conductive polymer should

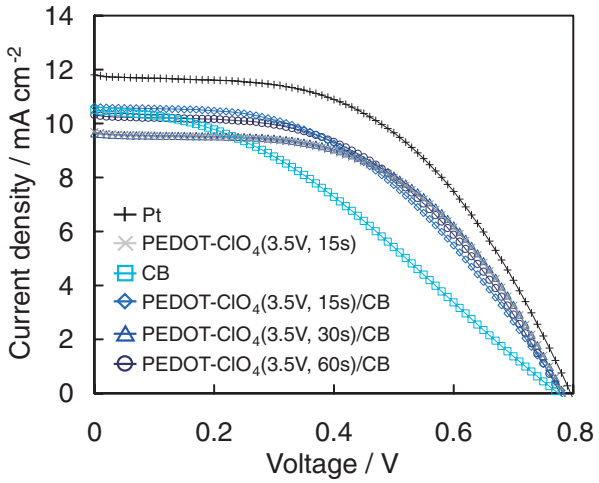

Figure 6. Photocurrent–voltage characteristics of DSSCs with various counter electrodes. The measurements were carried out under irradiation by a solar simulator (AM1.5, 100 mW cm^{-2}) powered by a Xe lamp with an air mass filter.

Table 3. Performance of DSSCs with Various Counter Electrodes

	J_{sc} /mA cm^{-2}	V_{oc} /V	Fill factor	Efficiency /%
Pt	11.81	0.79	0.52	4.86
PEDOT–ClO_4^-(3.5 V, 15 s)	9.69	0.78	0.53	4.00
CB	10.51	0.77	0.36	2.92
PEDOT–ClO_4^-(3.5 V, 15 s)/CB	10.63	0.78	0.47	3.88
PEDOT–ClO_4^-(3.5 V, 30 s)/CB	9.64	0.78	0.54	4.05
PEDOT–ClO_4^-(3.5 V, 60 s)/CB	10.32	0.78	0.50	4.01

promote electrical conduction. The R_s values of all PEDOT–ClO_4^-/C composite film electrodes were also smaller than that of the PEDOT–ClO_4^-(3.5 V, 15 s) film electrode. Therefore, the introduction of a PEDOT–ClO_4^- layer was extremely effective at improving the performance of the C particle film electrode.

Photocurrent–Voltage Characteristics of DSSCs with Various Counter Electrodes. As mentioned above, the as-prepared PEDOT–ClO_4^-/C particle film electrodes demonstrated superior performance to the C particle film electrode, according to electrochemical evaluations. Therefore, we investigated the photoelectric conversion efficiency of DSSCs with PEDOT–ClO_4^-/C composite film counter electrodes, based on their *I–V* characteristics. The results are shown in Figure 6, and the parameters evaluated using a fitting procedure are listed in Table 3.

As shown in Table 3, the fill factor (*FF*) values of DSSCs with C particle film and PEDOT–ClO_4^-/C composite film electrodes were 0.36 and 0.47, respectively. The *FF* values were greatly enhanced by the slight introduction of PEDOT–ClO_4^- to a C particle film electrode. The higher *FF* values of DSSCs with PEDOT–ClO_4^-/C composite film electrodes may have led to their higher performance, which was 33% higher than that of the DSSC with a C particle film electrode. Photocurrent–voltage characteristic experiments revealed that the DSSC with a PEDOT–ClO_4^-(3.5 V, 30 s)/C composite film electrode exhibited the highest performance ($\eta = 4.05\%$) among the composite film electrodes studied. Accordingly, the conversion efficiency of an as-prepared DSSC with a PEDOT–ClO_4^-(3.5 V, 30 s)/C composite film electrode was slightly lower than that of a DSSC with a deposited Pt counter electrode.

In addition, the UV–vis–diffuse reflection spectra indicate that visible light was little reflected from the surface of the PEDOT–ClO_4^-/C composite film counter electrode, but was partially reflected from the surface of the PEDOT–ClO_4^- film similar to Pt deposited film (data not shown). This difference of performance appeared to be caused by the absorption at the working electrode of light which had reflected from the surface of the counter electrode.

In a previous paper,[14] a similar experiment using PEDOT–ClO_4^-/TiO_2 composite film as a counter electrode material has been performed. In that case, TiO_2 particles were sintered to improve the electron conductivity and the strength of TiO_2 particulate film. Further improvement of the electron conductivity was carried out by using an electrically conductive C particle instead of TiO_2. Unfortunately, the further improvement of cell performance with PEDOT–ClO_4^-/C composite film was not achieved. This suggests that the conductive network structure of C particle due to poly(vinylpyrrolidone) without thermal treatment could not be formed. However, the PEDOT–ClO_4^-/C composite film was greatly improved from the viewpoint of strength and detachment of film, compared with the PEDOT–ClO_4^- film.

When a PEDOT–ClO_4^-(3.5 V, 15 s) film electrode was used, the performance was nearly equal to that of a deposited Pt film electrode. This higher performance was also due to the absorption of light reflected from the surface of the PEDOT–ClO_4^- film counter electrode. Therefore, PEDOT–ClO_4^-(3.5 V, 30 s)/C composite films provide the possibility of reducing the cost of dye-sensitized solar cells, compared with a deposited Pt film electrode.

Conclusion

PEDOT–ClO_4^-/C composite film electrodes were successfully prepared by an electrophoretic method and applied to the counter electrode of a dye-sensitized solar cell. The performance of this solar cell was greatly enhanced, compared with that of a cell based on a C particle film electrode. This led to an improved *FF* of the dye-sensitized solar cell with a PEDOT–ClO_4^-/C composite film counter electrode. In particular, when a PEDOT–ClO_4^-(3.5 V, 30 s)/C composite film electrode was used as a counter electrode, a conversion efficiency of 4.05% was obtained. This suggests that the introduction of PEDOT–ClO_4^- significantly improved the C particle film electrode. Therefore, PEDOT–ClO_4^-/C composite film counter electrodes may enable significant reduction in the cost of dye-sensitized solar cells.

This work was partially supported by a Grant-in-Aid for Scientific Research (C) (No. 20550166) from the Ministry of Education, Culture, Sports, Science and Technology.

References

1 B. O'Regan, M. Grätzel, *Nature* **1991**, *353*, 737.

2 M. K. Nazeeruddin, A. Kay, I. Rodicio, R. Humphry-Baker, E. Müller, P. Liska, N. Vlachopoulos, M. Grätzel, *J. Am. Chem. Soc.* **1993**, *115*, 6382.

3 T. N. Murakami, M. Grätzel, *Inorg. Chim. Acta* **2008**, *361*, 572.

4 Z. Huang, X. Liu, K. Li, D. Li, Y. Luo, H. Li, W. Song, L. Q. Chen, Q. Meng, *Electrochem. Commun.* **2007**, *9*, 596.

5 M.-Y. Yen, C.-Y. Yen, S.-H. Liao, M.-C. Hsiao, C.-C. Weng, Y.-F. Lin, C.-C. M. Ma, M.-C. Tsai, A. Su, K.-K. Ho, P.-L. Liu, *Compos. Sci. Technol.* **2009**, *69*, 2193.

6 E. Ramasamy, W. J. Lee, D. Y. Lee, J. S. Song, *Electrochem. Commun.* **2008**, *10*, 1087.

7 S. Gagliardi, L. Giorgi, R. Giorgi, N. Lisi, T. D. Makris, E. Salernitano, A. Rufoloni, *Superlattices Microstruct.* **2009**, *46*, 205.

8 J. Xia, N. Masaki, K. Jiang, S. Yanagida, *J. Mater. Chem.* **2007**, *17*, 2845.

9 Y. Saito, W. Kubo, T. Kitamura, Y. Wada, S. Yanagida, *J. Photochem. Photobiol., A* **2004**, *164*, 153.

10 T. Yohannes, O. Inganäs, *Sol. Energy Mater. Sol. Cells* **1998**, *51*, 193.

11 J.-G. Chen, H.-Y. Wei, K.-C. Ho, *Sol. Energy Mater. Sol. Cells* **2007**, *91*, 1472.

12 M. Biancardo, K. West, F. C. Krebs, *J. Photochem. Photobiol., A* **2007**, *187*, 395.

13 J. Wu, Q. Li, L. Fan, Z. Lan, P. Li, J. Lin, S. Hao, *J. Power Sources* **2008**, *181*, 172.

14 S. Sakurai, H. Q. Jiang, M. Takahashi, K. Kobayashi, *Electrochim. Acta* **2009**, *54*, 5463.

15 W. Xu, H. Chen, H. Li, M. Wang, *Colloids Surf., A* **2005**, *266*, 68.

16 Q. Wang, J. E. Moser, M. Grätzel, *J. Phys. Chem. B* **2005**, *109*, 14945.

17 R. Kern, R. Sastrawan, J. Ferber, R. Stangl, J. Luther, *Electrochim. Acta* **2002**, *47*, 4213.

18 A. Hauch, A. Georg, *Electrochim. Acta* **2001**, *46*, 3457.

19 L. Han, N. Koide, Y. Chiba, T. Mitate, *Appl. Phys. Lett.* **2004**, *84*, 2433.

20 L. Han, N. Koide, Y. Chiba, A. Islam, R. Komiya, N. Fuke, A. Fukui, R. Yamanaka, *Appl. Phys. Lett.* **2005**, *86*, 213501.